ACI MATERIALS JOURNAL TECHNICAL PAPER

Title no. 105-M28

Corrosion Resistance Performance of Steel-Reinforced Engineered Cementitious Composite Beams

by Mustafa Sahmaran, Victor C. Li, and Carmen Andrade

This paper presents the results of an experimental investigation on steel-reinforced engineered cementitious composite (ECC) beams subjected to accelerated corrosion by an electrochemical method. ECC is a micromechanically-based designed, high-performance, fiber-reinforced cementitious composite with high ductility and improved durability due to tight crack width. An accelerated corrosion test method, which was carried out by imposing a constant potential, was used to induce different degrees of corrosion into the reinforcement embedded in ECC prismatic specimens. Mortar specimens that have an equal compressive strength to the ECC specimens were also used as reference specimens. After inducing different degrees of accelerated corrosion, the cracks and the residual flexural load capacity of the test specimens and the mass loss of reinforcing bars embedded in specimens were determined. From the results of this study, it is concluded that due to its high tensile strain capacity and microcracking behaviors, ECC significantly prolonged the corrosion propagation period while enhancing the ability to maintain the load capacity of the beam. These performances of reinforced ECC (R/ECC) are expected to contribute substantially to improving infrastructure sustainability by reducing the amount of repair and maintenance during the service life of the infrastructure.

Keywords: corrosion; cracking; engineered cementitious composite; residual load capacity.

INTRODUCTION

The corrosion of reinforcing bars is one of the main causes of early deterioration of concrete structures, resulting in the reduction of their service life. Recent life-cycle analyses indicate that substantial material resource consumption, primary energy usage, and CO_2 emission occur during the service life of bridge infrastructure systems due to repeated maintenance activities.[1] Reducing corrosion-induced damage, therefore, is expected to contribute to the development of sustainable infrastructure systems.

Reinforcing steel bars embedded in concrete are usually well protected against corrosion by the high alkalinity of pore water because the steel surface is passivated in the presence of oxygen. Reinforcing steel bars in concrete structures, however, are depassivated when the chloride concentration reaches threshold levels on the reinforcing bar surface or when the pH of the concrete cover drops below critical levels due to carbonation.[2] When corrosion is initiated, active corrosion results in a volumetric expansion of the rust around the reinforcing bars against the surrounding concrete.[2] As a result, longitudinal corrosion cracks may form in the concrete along the corroding reinforcing bar due to the corrosion-induced tensile hoop stress, and repair or rehabilitation is usually required at this stage of structural deterioration.

Reinforced concrete (RC) structures require the use of innovative protective methodologies, generally divided into two categories. First, protection is attained through methods that delay the initiation of corrosion. The second approach includes methods that extend the active corrosion period, the period between corrosion initiation, and end of service life. For RC structures, durability design strategies generally seek to extend the initiation period as much as possible because the control of corrosion after initiation period is extremely difficult.

Some of the most commonly used protection methods for new construction against steel reinforcement corrosion include high-quality (low water-cement ratio [*w*/*c*] and good consolidation) concrete, increased concrete cover thickness, and use of epoxy-coated steel reinforcing bars. Generally, a low *w*/*c* and good consolidation contribute to the reduction in permeability. A larger cover thickness is supposed to provide better physical protection because the concrete acts as a barrier, which delays access of chloride ions, carbon dioxide, and moisture to the steel reinforcement. As a result of restrained shrinkage, thermal deformations, chemical reactions, poor construction practices, and mechanical loads, however, concrete unavoidably cracks and, over time, chlorides, carbon dioxide, and moisture can penetrate even high-quality concrete or concrete with good cover thickness.[3] In addition, a larger cover thickness is known to lead to a greater crack width. In addition, epoxy coatings on the surface of steel reinforcing bars are sometimes damaged during handling, or become brittle and delaminate from the steel reinforcing bars under high chloride concentrations so that the reliability of epoxy coating for steel protection has been called into question.[4-6] Consequently, corrosion of reinforcement occurs, which could lead to cover spalling and steel diameter reduction, and potential diminishing of the load capacity of the RC member. At the root of this steel corrosion problem is the brittle nature of concrete materials. The brittleness of concrete inherently results in cracks that allow corrosives to penetrate the cover, and fail to resist the expansive force once corrosion starts.

An engineered cementitious composite (ECC) is a ductile fiber-reinforced cementitious composite designed to achieve high damage tolerance under severe loading and high durability under normal service conditions.[7-9] Unlike ordinary concrete materials, ECC strain-hardens after first cracking, similar to a ductile metal, and demonstrates a strain capacity 300 to 500 times greater than normal concrete. Even at large imposed deformation, crack widths of ECC remain small—less than 100 μm (0.004 in.). The intrinsically tight crack width of ECC has been shown to be important to the high durability of infrastructure.

ACI Materials Journal, V. 105, No. 3, May-June 2008.
MS No. M-2006-505.R1 received May 13, 2007, and reviewed under Institute publication policies. Pertinent discussion including authors' closure, if any, will be published in the March-April 2009 *ACI Materials Journal* if the discussion is received by December 1, 2008.

ACI member **Mustafa Sahmaran** *is an Assistant Professor in the Department of Civil Engineering at the University of Gaziantep, Turkey. He is a member of ACI Committee 237, Self-Consolidating Concrete. His research interests include concrete technology, durability of concrete, and composite materials development for sustainable infrastructure.*

ACI member **Victor C. Li** *is a Professor in the Department of Civil and Environmental Engineering at the University of Michigan, Ann Arbor, MI. He is a member of ACI Committee 544, Fiber Reinforced Concrete. His research interests include the design of ultra-ductile and green cementitious composites and their application to innovative infrastructure systems, and integration of materials and structural design.*

Carmen Andrade *is a Research Professor at the High Research Council of Spain (CSIC) and is the Director of the Institute of Construction Science Eduardo Torroja. Her research interests include reinforcement durability, the assessment of steel corrosion, and repair and rehabilitation.*

Preliminary work has been performed on the transport of corrosives (initiation stage) through microcracked ECC by permeation. It has been found that cracked ECC exhibits nearly the same permeability as sound concrete, even when strained in tension to several percent.[10] Further, the effective chloride diffusivity in microcracked ECC is found to be substantially lower than cracked concrete subjected to the same amount of preloading.[11] With a tensile ductility of the order of 3 to 5%, cover spalling can be suppressed when concrete is replaced by ECC.[12] By preserving low transport properties especially after cracking, and without spalling, the ability of ECC material to effectively protect reinforcement from corrosion significantly longer than concrete is expected. This protection concept is further supported by recent research by Miyazato and Hiraishi[13] in which ECC material was found to be effective in reducing the chloride penetration depth as well as the rate of corrosion of steel embedded in ECC after cracking when compared with normal concrete.

With an intrinsically tight crack width and high tensile ductility, ECC offers a significant potential to naturally resolving the corrosion-related durability problem of RC structures. The focus of the present study is on the performance of ECC after corrosion is initiated. Specifically, the cracking behavior and residual flexural load capacities of reinforced ECC (R/ECC) specimens subjected to accelerated corrosion at constant applied voltage were experimentally investigated.

Table 1—Mechanical and geometrical properties of PVA fiber

Nominal strength, MPa (ksi)	Apparent strength, MPa (ksi)	Diameter, μm (in.)	Length, mm (in.)	Young's modulus, GPa (ksi)	Elongation, %
1620 (235)	1092 (158)	39 (0.002)	8 (0.3)	42.8 (6200)	6.0

Table 2—Mixture properties of ECC and mortar

	ECC (M45)	Mortar
FA/C	1.2	—
w/cm	0.27	0.35
Water, kg/m^3 (lb/yd^3)	331 (558)	215 (362)
Cement, kg/m^3 (lb/yd^3)	570 (961)	614 (1035)
Fly ash, kg/m^3 (lb/yd^3)	684 (1153)	—
Sand, kg/m^3 (lb/yd^3)	455 (767)	1535 (2585)
Fiber (PVA), kg/m^3 (lb/yd^3)	26 (44)	—
High-range water-reducing admixture, kg/m^3 (lb/yd^3)	4.9 (8.3)	—
7-day compressive strength, MPa (ksi)	38.1 (5.5)	38.4 (5.6)
28-day compressive strength, MPa (ksi)	50.2 (7.3)	49.0 (7.1)
7-day tensile strain capacity, %	3.48	—
28-day tensile strain capacity, %	3.16	—

RESEARCH SIGNIFICANCE

The corrosion of steel reinforcement in aging infrastructure is one of the main problems currently facing the civil engineering community. In the U.S., maintenance and replacement costs are measured in billions of dollars. These costs are a tremendous burden on the economies of the U.S. and other countries. To reduce this burden, the service life of RC infrastructure needs to be substantially enhanced. ECC is a ductile fiber-reinforced cementitious composite developed to achieve high damage tolerance under severe mechanical and environmental loading while maintaining inherently extreme tight crack width. This study investigates the performance of R/ECC beams under a corrosive environment. Experimental test results will be used to validate the failure resistance of R/ECC, even when corrosion of reinforcement is artificially induced. Findings from this research provide the technical basis for using ECC to extend infrastructure service life and reduce maintenance costs.

EXPERIMENTAL STUDIES

Materials, mixture proportions, and basic mechanical properties

The materials used in the ECC mixture were ordinary portland cement (OPC); Class F fly ash (FA) with a lime content of 10.44%; silica sand with an average and maximum grain size of 110 and 200 μm (0.004 and 0.008 in.), respectively; water; polyvinyl alcohol (PVA) fibers; and a high-range water-reducing admixture (HRWRA). The PVA fibers were purposely manufactured with a tensile strength, elastic modulus, and maximum elongation needed for composite strain-hardening performance. Additionally, the surface of the PVA fibers was coated with a proprietary oiling agent 1.2% by weight to tailor the interfacial properties between the fiber and the cementitious matrix for strain-hardening performance.[14] The mechanical and geometrical properties of the PVA fibers used in this study are shown in Table 1.

The mixture proportions for ECC (M45) are summarized in Table 2. The ECC mixture was prepared in a mixer with a 12 L (12.7 qt) capacity. Solid ingredients, including cement, fly ash, and sand, were first mixed at 100 rpm for 1 minute. Water and chemical admixtures were then added into the dry mixture and mixed at 300 rpm for 3 minutes to produce a consistent and uniform mortar and then PVA fiber was added in last and mixed at 150 rpm for an additional 3 minutes. In a control test series, a mortar mixture with a similar compressive strength to the ECC mixture was included. The mixture proportions of the mortar are also shown in Table 2.

The compressive strength test results of ECC and mortar mixtures and the ultimate tensile strain capacity of ECC at 7 and 28 days are listed in Table 2. The companion cylinders with 75 mm (3 in.) diameter and 150 mm (6 in.) height were tested following the standard ASTM C39 procedures. A minimum of three compression cylinders were used to obtain the average compressive strengths. To characterize the direct tensile behavior of ECC, 152 x 76 x 13 mm (6.0 x 3.0 x 0.5 in.) coupon specimens were used. Direct tensile tests were conducted under displacement control at a loading rate of 0.005 mm/s (0.0002 in./s). The tensile stress-strain curves of ECC at 7 and 28 days are shown in Fig. 1. This ECC composite exhibited a strain capacity more than 3.0% at 28 days. The

strain capacity measured after 28 days was slightly lower than the 7-day strain capacity; however, the observed 3.0% strain capacity remained acceptable for an ECC.

From each mixture, 255 x 75 x 50 mm (10 x 2 x 3 in.) prism specimens with a centrally placed deformed steel bar that had a 13 mm (0.512 in.) diameter (No. 4, Grade 60, ASTM A615) and a length of 300 mm (11.81 in.) were prepared for the accelerated corrosion test. Steel bars were cleaned with a wire brush to remove any rust from the surface just before casting the reinforced specimens. At the air/mortar interface, the steel bars were coated with epoxy glue to avoid crevice corrosion. All specimens were demolded at 24 hours and moisture-cured in plastic bags at 95 ± 5% relative humidity (RH) and 23 ± 2 °C (73 °F) for 7 days. The prism specimens were then air-cured in laboratory medium at 50 ± 5% RH and 23 ± 2 °C (73 °F) until 28 days for testing.

Accelerated reinforcement corrosion

An accelerated corrosion testing technique[15,16] was used to compare the corrosion performance of mortar and ECC. At the end of 28 days, the ECC and mortar prism specimens with a centrally placed steel bar were partially immersed in a 5% NaCl solution, as shown in Fig. 2. The exposed steel bar was then connected to the positive terminal of a DC power source while the negative terminal was connected to stainless steel plates placed near the specimen in the solution. The weight of the steel bar was measured and recorded for weight loss measurement before accelerated corrosion test. The corrosion process was initiated by applying a constant 30 V anodic potential. High voltage was used to accelerate the corrosion and shorten the test period. Similar accelerated corrosion test setups were also used by other researchers.[17-22] Samples were visually inspected for cracks daily while the current flow was continuously monitored. The current increased suddenly whenever the specimen cracked. The widths of the crack were also measured regularly on the surface of the specimens by an optical microscope.

For the 28-day residual flexural load test (Fig. 3), ECC and mortar specimens with a 50 x 75 mm (2 x 3 in.) cross section, 255 mm (10 in.) in length, a support span length of 225 mm (8.85 in.), and a center span length of 75 mm (2.95 in.) were tested in a closed-loop machine after having been exposed to different degrees of accelerated corrosion (Table 3). In each case, two replica specimens were loaded until failure to determine their load-deflection curves and ultimate flexural load capacity. Three control prisms of each mixture without accelerated corrosion exposure were also tested after 28 days curing as references.

Table 3—Ultimate flexural load at different degrees of accelerated corrosion level

Mixture ID	Accelerated time, hours	Ultimate flexural load, kN (kip)	Failure type	No. of specimens
Mortar	—	15.12 (3.40)	Shear	3
	25	5.61 (1.26)	Bond	2
	50	4.93 (1.11)	Bond	2
	75	4.65 (1.05)	Bond	2
ECC (M45)	—	26.86 (6.04)	Bending	3
	50	26.05 (5.86)	Bending	2
	100	22.13 (4.98)	Bending	2
	150	16.18 (3.64)	Bending	2
	300	11.70 (2.63)	Bending	2

RESULTS AND DISCUSSION

Corrosion current and cracking behavior

During accelerated corrosion, it is assumed that the electrical potential applied to the reinforcement attracted negatively-charged chloride ions from the solution into the concrete and toward the positively charged steel bars. As the chloride ions reached the steel-concrete interface above threshold concentration, the steel surface began to corrode. The expansive products of corrosion-imposed tensile stresses on the mortar/

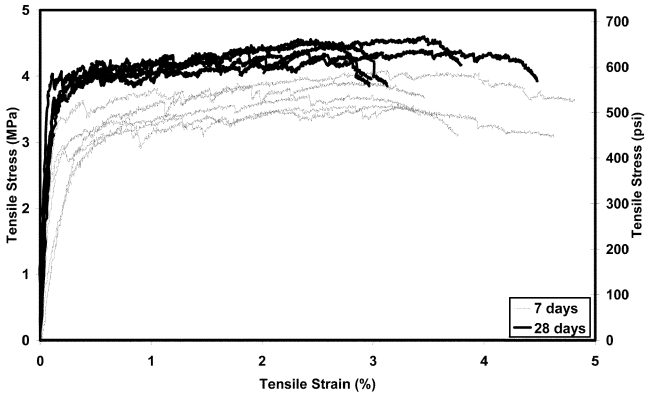

Fig. 1—Tensile behavior of ECC.

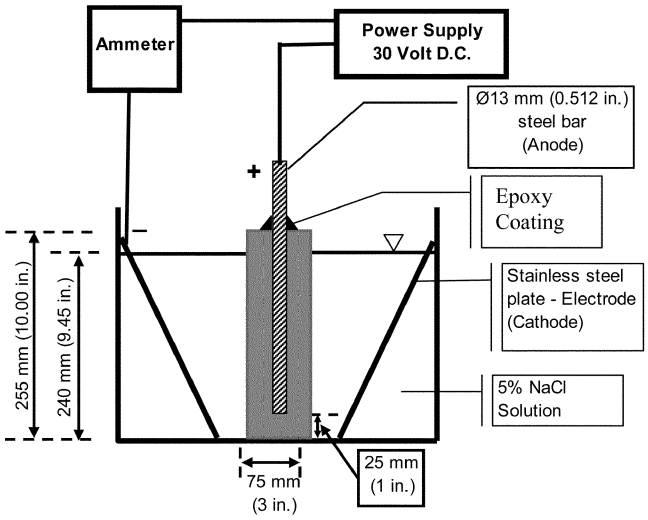

Fig. 2—Accelerated corrosion test setup.

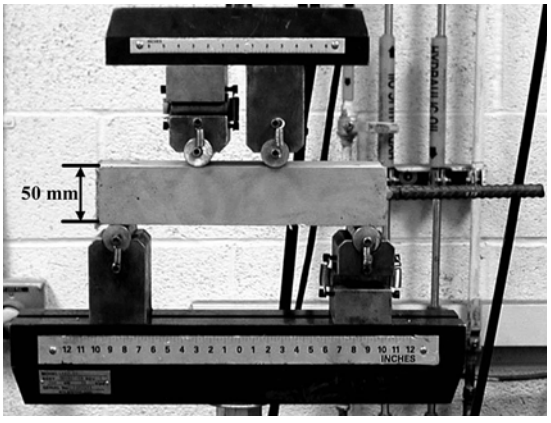

Fig. 3—Flexural test setup.

ECC cover resulted in cracking when the tensile stresses exceeded the tensile strength of the cover material. Cracking, especially large cracks, would allow the conductive chloride solution to come into direct contact with the steel surface, thus providing a direct current path between the reinforcement and the electrodes in solution. Therefore, a current spike, or a dramatic increase in current flow, suggests a reduction in electrical resistance following cracking in the cementitious material around the steel bar.

The current response as a function of time under the fixed potential is shown in Fig. 4. Each line in Fig. 4 is the average of three specimens. The current-time curves were used to determine the time to initiation of reinforcement corrosion by observing any instantaneous rise in the current recorded.

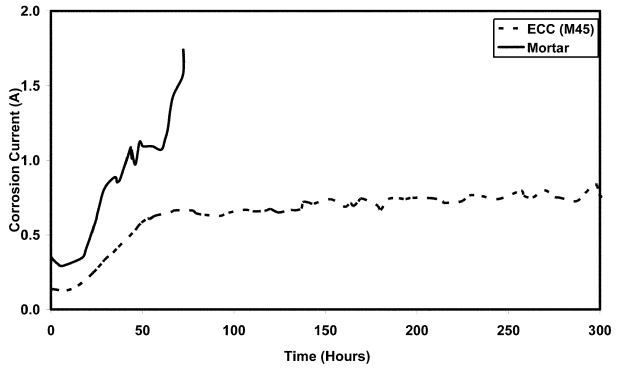

Fig. 4—Measured corrosion current with time for ECC and mortar specimens.

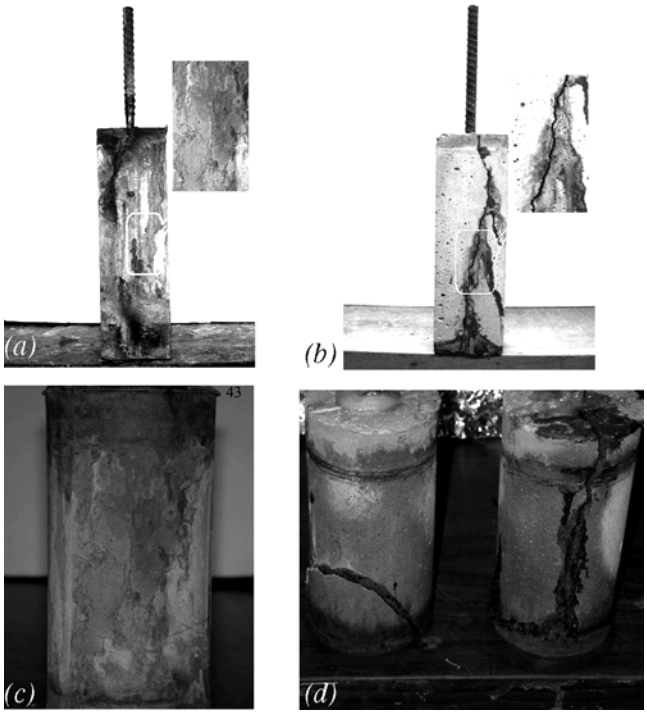

Fig. 5—ECC and mortar specimens after accelerated corrosion test: (a) ECC prismatic specimen after 300 hours of accelerated corrosion; (b) mortar prismatic specimen after 75 hours of accelerated corrosion; (c) ECC cylindrical specimen after 350 hours of accelerated corrosion; and (d) mortar cylindrical specimen after 95 hours of accelerated corrosion.

As seen from Fig. 4, the current recorded for the mortar specimens remained approximately 0.4 A up until approximately 20 hours and then a rapid increase in current was detected. The sudden rise of the current intensity coincided with the observation of a 0.3 mm (0.012 in.) size crack width on the mortar specimens. The current recorded for the ECC specimens was much lower, at approximately 0.2 A up until 15 to 20 hours. The lower initial current recorded in the ECC specimens compared with the mortar specimens may reflect the higher electrical resistivity of the ECC.

In general, each of the current responses and corrosion rates of the material is considered to be inversely proportional to the electrical resistivity of the material.[23,24] In addition, according to Andrade et al.,[25] the inverse of resistivity is proportional to the chloride diffusion coefficient in concrete materials and, therefore, the corrosion initiation period. For ECC, a lower water-cementitious material ratio (*w/cm*) and high-volume fly ash (FA), resulting in a denser matrix by reducing the pore sizes and thickness of the transition zone between the fiber and the surrounding cementitious matrix, may explain the observed higher electrical resistivity.[26-27] This higher electrical resistivity of ECC is expected to be associated with a longer corrosion initiation period under field conditions.

As the experiment is continued, the recorded current (and the corrosion of the steel bar) steadily increased in the ECC specimens until approximately 50 hours. Microcracking on the surface of these specimens was first noted after 35 hours. Beyond 50 hours, the recorded current became more or less steady until the failure (defined in the following as when the crack width reaches 0.3 mm [0.012 in.])[28] of the ECC specimens. In contrast to the mortar specimens, localized large cracks were not observed in the ECC specimens. Instead, a distribution of microcracks was observed. The tight crack width (see following paragraph) of the surrounding ECC did not allow easy access of the moisture[10] and chloride ions[11] to the surface of the steel bars embedded in the ECC specimens. In addition, self-healing[11] and potentially plugging of these microcracks by corrosion products may have occurred. Microcracks tend to be easier to seal than large cracks, thus prolonging the corrosion propagation period. This increase in the accelerated corrosion propagation time indicates a superior durability performance of ECC over mortar. Whereas the increase in the number of microcracks tends to lower the resistivity of the specimen, the plugging of these cracks that stabilize in width below 100 μm (0.004 in.) is likely responsible for the steady state current observed beyond 50 hours in Fig. 4.

The typical surface patterns of corrosion-induced cracks for mortar and ECC specimens after subjected to accelerated corrosion test are shown in Fig. 5. In addition to prism specimens, the cracking resistance of cylindrical specimens (75 mm [3 in.] in diameter and 150 mm [6 in.] in height) with a centrally placed deformed steel bar that have a 13 mm (0.512 in.) diameter was measured by using the same test setup. As seen in Fig. 5, the cracking behavior was significantly different between ECC and mortar. One longitudinal crack formed on each of the wider faces of the beam (the faces 75 mm [3 in.] wide) directly adjacent to the reinforcing bar and parallel to the reinforcement along its length was observed for the mortar (Fig. 5(b)). These were typical corrosion-induced cracks caused by the circumferential tensile stresses due to the expansive corrosion products. The crack width of the mortar specimens increases with increasing corrosion

exposure time. The maximum corrosion crack width was recorded at the end of the 75 hours, at approximately 2.00 mm (0.079 in.). In addition to longitudinal cracks, cover spalling was also observed in the cylindrical mortar specimens after 95 hours of accelerated corrosion (Fig. 5(d)).

On the other hand, multiple microcracks on the two wider faces of the ECC beams were observed (Fig. 5(a)). The number of microcracks on the surface of ECC specimens increased as corrosion progressed. This could be attributed to the strain-hardening and multiple-cracking behaviors of the ECC. After 150 hours of accelerated corrosion, numerous (at least 10) microcracks with widths less than 0.1 mm (0.004 in.) were observed on each surface of the ECC specimens. Similar behavior was observed in the ECC cylinder specimens (Fig. 5(c)). This implies that ECC maintains substantial resistance against cover spalling in R/ECC members in the presence of significant steel bar corrosion.

At the end of 300-hour accelerated corrosion test, in addition to microcracks, one longitudinal localized crack with width of nearly 0.3 mm (0.012 in.) on the surface of the ECC prism specimens was observed. If a crack width of 0.3 mm (0.012 in.) is defined as a failure limit for RC structures, as, for example, suggested by an earlier version of the ACI Building Code[28] or AASHTO[29] for crack width limit for outdoor exposures, the service life duration of R/ECC will be at least 15 times that of the mortar specimens (300 hours for ECC versus 20 hours for mortar prism specimens under accelerated corrosion conditions). This indicates that ECC significantly extends service life (time to corrosion initiation plus time to corrosion propagation) under accelerated test conditions.

Mass loss measurements

To measure the mass loss of the reinforcing steel, the specimens were broken to retrieve the entire reinforcing bar after inducing different degrees of accelerated corrosion exposures. The reinforcing bar for each specimen was cleaned with deionized water and scrubbed with a stiff metal brush to ensure that the bar was free from any adhering corrosion products. The reinforcing bar was then weighed and the percentage mass loss was computed using Eq. (1)

$$\text{corrosion mass loss} = \frac{[\text{initial mass} - \text{final mass}]}{\text{initial mass}} \times 100 \quad (1)$$

where the initial and final mass refer to the mass of the reinforcing bars before and after corrosion exposures.

The percentage of steel mass losses of the ECC and mortar beams at different accelerated corrosion exposures is presented in Fig. 6. The average percentage of mass losses of reinforcing bars embedded in the mortar specimens were 2.5%, 5.3%, and 11.7% at the end of 25, 50, and 75 hours of accelerated corrosion exposure, respectively. On the other hand, there was nearly no mass loss of reinforcing bars embedded in the ECC specimens up to 50 hours of accelerated corrosion exposure. The average percentage of mass loss was 17.5% at the end of 300 hours of accelerated corrosion exposure.

To appreciate the difference in the rate of corrosion between the ECC and mortar specimens, the percent mass loss rate is shown in Fig. 7. Examining the mass loss per hour of exposure at the end of the tests provides a rough measure of the overall rate of corrosion for the entire specimen life span. It also serves to normalize the mass loss data because the ECC and mortar specimens were given different accelerated corrosion exposure time periods. ECC samples exposed to 300 hours accelerated corrosion showed approximately 41% less mass loss per hour averaged over the service life than the mortar samples exposed to 20 hours accelerated corrosion. The reason that the mortar beams exhibited higher measured mass loss rate values than that of the ECC beams is because of the wide longitudinal cracks formed along the complete length of the beam, which leads to increased accessibility for water[10] and chloride ions.[11] The cracks were wide enough to allow easy migration of corrosion products, seen as rust on the crack surfaces of the severely damaged specimens (Fig. 5(b) and (d)). For the ECC beams, the tight crack width inhibits movements of the corrosion products that serve as a shield against chloride ion migration toward the steel bar. Therefore, ECC cover reduces the corrosion rate of steel reinforcement significantly when compared with a mortar cover, at least under the present accelerated test conditions.

Residual flexural load

After inducing different degrees of accelerated corrosion, the corroded beams were tested under four-point bending (Fig. 3) to determine their residual load-deflection curves and ultimate flexural loads. Bending loads were applied to the wider face of the beam (the face was 75 mm [3 in.] wide) where corrosion-induced cracks were observed. Such a loading arrangement allows for a more realistic evaluation of the residual flexural load capacity of corroded specimens because, in the case of the bridge decks exposed to deicing salts, mechanical loads are generally applied on the surfaces where cracks are present.

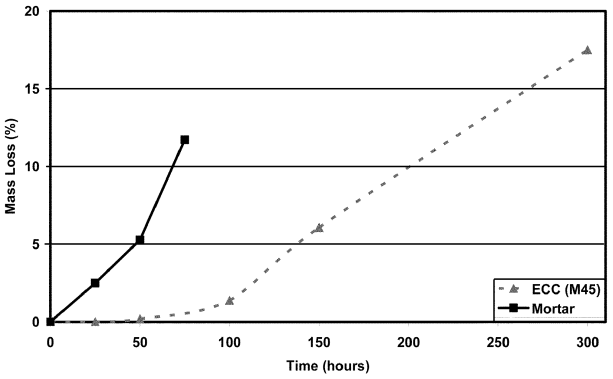

Fig. 6—Mass loss versus corrosion exposure time for ECC and mortar corrosion specimens.

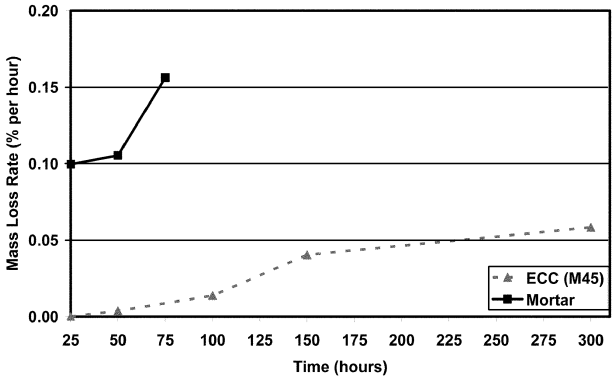

Fig. 7—Mass loss rate (mass loss per hour) of ECC and mortar corrosion specimens.

The ultimate flexural load of the deteriorated (with corrosion) and control (without corrosion) specimens with their failure types at each selected degree of accelerated corrosion level is summarized in Table 3. Average ultimate flexural loads for the beam specimens were obtained by combining the results of two or three specimens tested in each case. The averaged ultimate flexural loads were 26.86 and 15.12 kN (6.04 and 3.40 kip) for ECC and mortar, respectively. The ECC beams show a substantially higher ultimate flexural load in comparison with that of the mortar beams. ECC specimens showed multiple cracking behaviors with small crack spacing and tight crack widths (<0.1 mm [0.004 in.]). Bending failure in the ECC occurred when the fiber bridging strength at one of the microcracks was reached, resulting in localized deformation at this section (Fig. 8(a)). Previous study has also showed that ECC beams without shear reinforcement exhibits remarkable shear resistance because of its strain-hardening and multiple-cracking behaviors under tensile loads.[30] On the other hand, because of the low tensile properties and the lack of shear reinforcement, control mortar beams failed by shear under the four-point bending test (Fig. 8(c)). The shear failure in mortar specimens can be prevented with stirrups (shear reinforcement); however, for the comparison purpose, stirrups were not used for either the ECC or the mortar specimens.

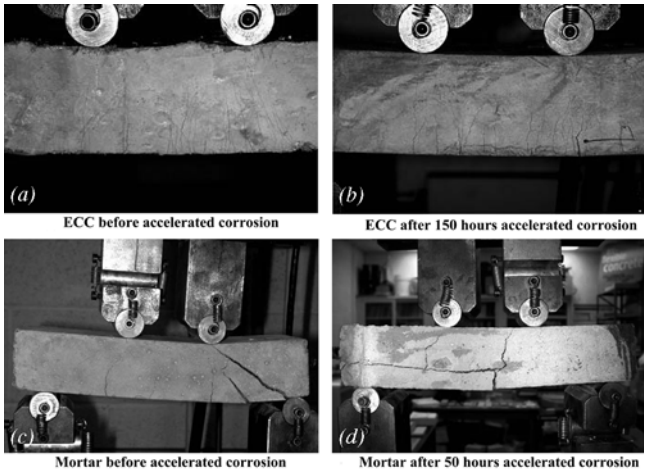

Fig. 8—Type of failure of mortar and ECC beams under four-point bending test before and after accelerated corrosion test.

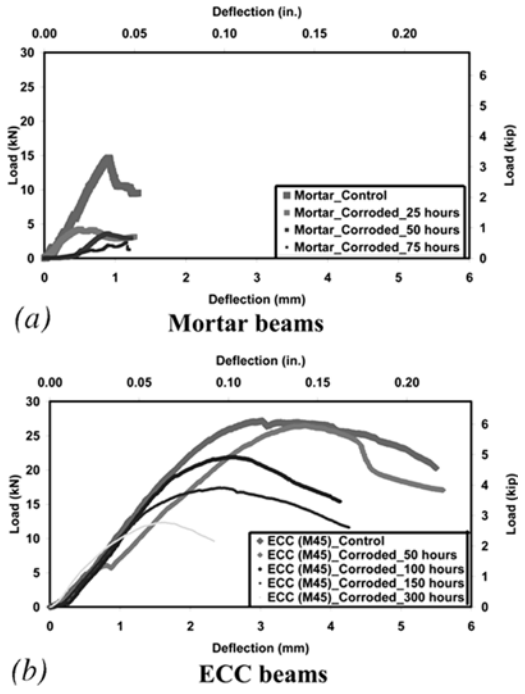

Fig. 9—Effect of accelerated corrosion on load-deflection curves.

Typical load-deflection curves of the mortar and ECC specimens before (control) and after different accelerated corrosion periods (corroded, *x* hours) are shown in Fig. 9. To facilitate the comparison between the test results for mortar and ECC beams, the same scales for both axes were used in these figures. Figure 9(a) shows that the effect of accelerated corrosion has a marked influence on the load-deflection curves of mortar specimens. The ultimate load capacity decreases sharply with an increasing accelerated corrosion period. For example, after a 25-hour accelerated corrosion test period, the residual flexural load is only 37% that of the control beams. The corrosion-induced longitudinal cracking along the reinforcing bar in the mortar specimens leads to a loss of frictional mechanical bond.[31] The slope of the load-deflection curve represents the stiffness of the beams and it can be easily noted from Fig. 9(a) that the slope decreases with an increasing degree of reinforcement corrosion, thereby indicating a significant reduction in the stiffness of the mortar beams. Corrosion of reinforcement also modified the type of failure in mortar beams. Control (without corrosion) mortar beams failed by shear; however, corroded mortar beams failed by bond splitting (Fig. 8(c) and (d)). The failure mechanism can be explained in terms of the bond between reinforcement and mortar being reduced by reinforcement corrosion to an extent that, as the load increased, transmission of stresses between the two materials gradually became concentrated at the beam ends where anchorage was provided by the bent portions of reinforcement.[32] These portions of reinforcement were not severely corroded because they were above the submerged level of the beams during the accelerated corrosion-inducing process.

The typical load-deflection curves of ECC specimens after accelerated corrosion shown in Fig. 9(b) reveal that the influence of accelerated corrosion test up to 50 hours on the load-deflection curves of the ECC specimen is fairly small. Beyond 50 hours of accelerated corrosion, the ultimate residual flexural load capacity of ECC specimens decreased slowly as corrosion progressed. This result was consistent with the earlier results of steel mass loss of ECC specimens (Fig. 6 and 7). The decrease in the ultimate flexural loads is attributed to the loss of the cross-sectional area of steel reinforcements and, in addition, to the presence of multiple microcracking. On the other hand, ECC deterioration due to the corrosion of reinforcement did not change the type of failure in ECC beams. Both corroded and control ECC beams failed in flexure (Fig. 8(a) and (b)).

The residual ultimate flexural load-deflection curve of corroded ECC beams presented in Fig. 9(b) provides a conservative estimate of their ultimate residual flexural load capacity in actual structures. This is because the effect of self-healing of microcracked ECC has not been included in these specimens due to the short experimental duration. Tuutti[2] proposed that cracks of width less than 0.1 to 0.3 mm (0.004 to 0.012 in.) did not affect the corrosion rate of the reinforcing steel. The residual flexural load capacity of the

ECC beams was determined following induced accelerated corrosion of the reinforced specimen during 50 to 300 hours. Such corrosion periods are equivalent to those of many years in real structures. This difference in accelerated and normal corrosion periods can have a significant influence on the residual flexural load of ECC. For long-term corrosion exposure, after corrosion initiates, microcracks in ECC generated by mechanical loading or corrosion expansion can easily be closed or become smaller and less connected among them due to self-healing,[11] thus slowing down further chloride penetration and reducing the rate of corrosion propagation.

The present accelerated corrosion experiment has been carried out by applying a constant potential to the specimens, as is typical of this type of investigation.[17-22] Because of the expected differences in electrical resistance between uncracked ECC and uncracked mortar, however, the generated currents may also be different. As a result, the rate of corrosion and mass loss rate data may reflect this difference and therefore should be interpreted with care. Even so, the tight crack width of ECC provides an effectively higher resistance material by limiting the access of chloride ions, carbon dioxide, and moisture to the reinforcing bar than that of mortar that has a much larger crack width. This results in a reduction of current (and therefore mass loss and corrosion rate), which is a real benefit of ECC over mortar. Regardless of the way the accelerated corrosion test was conducted, the mode of failure between ECC and mortar are substantially different.

CONCLUSIONS

Based on the results and analysis presented in this paper, the following conclusions can be drawn:

1. Corrosion-induced crack width of mortar specimens increases with time as corrosion activity progresses. Larger crack widths up to 2.00 mm (0.079 in.) are obtained at higher levels of corrosion. On the other hand, crack widths (~0.1 mm [0.004 in.]) of ECC remain nearly constant with time as corrosion activity progresses, whereas the number of cracks on the surface of the ECC specimens increased. The results of this study also showed that ECC has significant anti-spalling ability compared with conventional mortar. If a crack width of 0.3 mm (0.012 in.) is used to set a service time limit of RC structures, the service life of R/ECC will be at least 15 times as much as that of the reinforced mortar;

2. Corrosion of reinforced mortar specimens results in a marked reduction on stiffness and flexural load capacity. After 25 hours of accelerated corrosion exposure, the flexural load reduces to approximately 34% of the flexural capacity of the control mortar beam. In contrast, the ECC specimens, after 50 hours of accelerated corrosion exposure, retained almost 100% of the flexural capacity of the control specimens. Beyond 50 hours, the flexural capacity decreased, but retained over 45% that of the control specimens, even after 300 hours of accelerated corrosion exposure; and

3. Longitudinal cracks due to expansion of the corrosion products affect the failure mode of the reinforced mortar under four-point bend test. On the other hand, the corrosion of the steel bar in ECC specimens does not change the type of failure in ECC beams.

Finally, the observed superior corrosion resistance of ECC compared with mortar in terms of corrosion propagation time, tight crack width, lower weight loss, and higher retention of stiffness and flexural load, is attributable to the high tensile strain capacity, strain hardening, and multiple-cracking behaviors of ECC. Overall, these experimental findings suggest that the propagation period of corrosion could be safely included in estimating the service life of a structure when concrete is replaced by ECC.

ACKNOWLEDGMENTS

The first author would like to acknowledge the financial support of the Scientific and Technical Research Council of Turkey (TUBITAK). This research was partially funded through an NSF MUSES Biocomplexity Program Grant (CMS-0223971 and CMS-0329416). MUSES (Materials Use: Science, Engineering, and Society) supports projects that study the reduction of adverse human impact on the total interactive system of resource use, the design and synthesis of new materials with environmentally benign impacts on biocomplex systems, as well as the maximization of efficient use of materials throughout their life cycles.

REFERENCES

1. Keoleian, G. A.; Kendall, A.; Dettling, J. E.; Smith, V. M.; Chandler, R.; Lepech, M. D.; and Li, V. C., "Life Cycle Modeling of Concrete Bridge Design: Comparison of Engineered Cementitious Composite Link Slabs and Conventional Steel Expansion Joints," *Journal of Infrastructure Systems*, ASCE, V. 11, No. 1, Mar. 2005, pp. 51-60.

2. Tuutti, K., "Corrosion of Steel in Concrete," CBI Swedish Cement and Concrete Research Institute, Stockholm, Sweden, 1982, 159 pp.

3. ACI Committee 224, "Control of Cracking in Concrete Structures (ACI 224R-01)," American Concrete Institute, Farmington Hills, MI, 2001, 46 pp.

4. Federal Highway Administration, "Corrosion Detection in Reinforced Concrete Bridge Structures," Project 84, Washington, DC, 1992.

5. Sagues, A. A.; Powers, R. G.; and Locke, C. E., "Corrosion Processes and Field Performance of Epoxy-Coated Reinforcing Steel in Marine Structures," *Paper* No. 299, Corrosion 94, Houston, TX, 1994.

6. Manning, D. G., "Corrosion Performance of Epoxy-Coated Reinforcing Steel: North American Experience," *Construction and Building Materials*, V. 10, No. 5, 1996, pp. 349-365.

7. Li, V. C., "ECC—Tailored Composites through Micromechanical Modeling," *Fiber Reinforced Concrete: Present and the Future*, Banthia et al., eds., CSCE, Montreal, QC, Canada, 1998, pp. 64-97.

8. Li, V. C., "On Engineered Cementitious Composites (ECC)—A Review of the Material and its Applications," *Journal of Advanced Concrete Technology*, V. 1, No. 3, 2003, pp. 215-230.

9. Li, V. C.; Wang, S.; and Wu, C., "Tensile Strain-Hardening Behavior of PVA-ECC," *ACI Materials Journal*, V. 98, No. 6, Nov.-Dec. 2001, pp. 483-492.

10. Lepech, M. D., and Li, V. C., "Water Permeability of Cracked Cementitious Composites," *Compendium of Papers*, ICF 11, Turin, Italy, Mar. 2005. (CD-ROM)

11. Sahmaran, M.; Li, M.; and Li, V. C., "Transport Properties of Engineered Cementitious Composites under Chloride Exposure," *ACI Materials Journal*, V. 104, No. 6, Nov.-Dec. 2007, pp. 604-611.

12. Li, V. C., and Stang, H., "Elevating FRC Material Ductility to Infrastructure Durability," *Proceedings of BEFIB*, Varenna, Lake Como, Italy, Sept. 2004, pp. 171-186.

13. Miyazato, S., and Hiraishi, Y., "Transport Properties and Steel Corrosion in Ductile Fiber Reinforced Cement Composites," *Proceedings of the Eleventh International Conference on Fracture*, Turin, Italy, Mar. 2005. (CD-ROM)

14. Li, V. C.; Wu, C.; Wang, S.; Ogawa, A.; and Saito, T., "Interface Tailoring for Strain-Hardening PVA-ECC," *ACI Materials Journal*, V. 99, No. 5, Sept.-Oct. 2002, pp. 463-472.

15. NORDTEST, NT BUILD 356, "Concrete, Repairing Materials and Protective Coating: Embedded Steel Method, Chloride Permeability," Espoo, Finland, 1989, 3 pp.

16. Florida Department of Transportation (FDOT), "An Accelerated Laboratory Method for Corrosion of Reinforced Concrete Using Impressed Current," *Manual of Florida Sampling and Testing Methods*, Tallahassee, FL, 2000, 6 pp.

17. Al-Tayyib, A. J., and Al-Zahrani, M. M., "Corrosion of Steel Reinforcement in Polypropylene Fiber Reinforced Concrete Structure," *ACI Materials Journal*, V. 87, No. 2, Mar.-Apr. 1990, pp. 108-113.

18. Detwiler, R. J.; Kjellsen, K. O.; and Gjorv, O. E., "Resistance to Chloride Intrusion of Concrete Cured at Different Temperature," *ACI Materials Journal*, V. 88, No. 1, Jan.-Feb. 1991, pp. 19-24.

19. Shaker, F. A.; El-Dieb, A. S.; and Reda, M. M., "Durability of Styrene Butadiene Latex Modified Concrete," *Cement Concrete Research*, V. 27, No. 5, 1997, pp. 711-720.

20. Okba, S. H.; El-Dieb, A. S.; and Reda, M. M., "Evaluation of the Corrosion Resistance of Latex Modified Concrete (LMC)," *Cement and Concrete Research*, V. 27, No. 6, 1997, pp. 861-868.

21. Al-Zahani, M. M.; Al-Dulaijan, S. U.; Ibrahim, M.; Saricimen, H.; and Sharif, F. M., "Effect of Waterproofing Coating on Steel Reinforcement Corrosion and Physical Properties of Concrete," *Cement Concrete Composites*, V. 24, No. 1, 2002, pp. 127-137.

22. Sujjavanich, S.; Sida, V.; and Suwanvitaya, P., "Chloride Permeability and Corrosion Risk of High-Volume Fly Ash Concrete with Mid-Range Water Reducer," *ACI Materials Journal*, V. 102, No. 3, May-June 2005, pp. 177-182.

23. Bažant, Z., "Physical Model for Steel Corrosion in Concrete Sea Structures Part Theory Part Application," *Journal of the Structural Division*, ASCE, V. 105, No. ST6, 1979, pp. 1137-1166.

24. Smith, K. M.; Schokker, A. J.; and Tikalsky, P. J., "Performance of Supplementary Cementitious Materials in Concrete Resistivity and Corrosion Monitoring Evaluations," *ACI Materials Journal*, V. 101, No. 5, Sept.-Oct. 2004, pp. 385-390.

25. Andrade, C.; Sanjuan, M. A.; and Alonso, M. C., "Measurement of Chloride Diffusion Coefficient from Migration Tests," *Paper* No. 319, NACE Corrosion'93, 1993.

26. Hussian, S. E., and Rasheeduzzafar, M., "Corrosion Resistance Performance of Fly Ash Blended Cement Concrete," *ACI Materials Journal*, V. 91, No. 3, May-June 1994, pp. 264-272.

27. Sun, W.; Zhang, Y. S.; Liu, S. F.; and Zhang, Y. M., "The Influence of Mineral Admixtures on Resistance to Corrosion of Steel," *Journal of Cement and Concrete Research*, V. 34, No. 10, 2004, pp. 1781-1785.

28. ACI Committee 318, "Building Code Requirements for Structural Concrete (ACI 318-95) and Commentary (318R-95)," American Concrete Institute, Farmington Hills, MI, 1995, 369 pp.

29. AASHTO, "AASHTO LRFD Bridge Design Specifications," third edition, Washington, DC, 2004, 1450 pp.

30. Li, V. C., and Wang, S., "Flexural Behavior of GFRP Reinforced Engineered Cementitious Composite Beams," *ACI Materials Journal*, V. 99, No. 1, Jan.-Feb. 2002, pp. 11-21.

31. Amleh, L., and Mirza, S., "Corrosion Influence on Bond between Steel and Concrete," *ACI Structural Journal*, V. 96, No. 3, May-June 1999, pp. 415-423.

32. Mangat, P. S., and Elgarf, M. S., "Flexural Strength of Concrete Beams with Corroding Reinforcement," *ACI Structural Journal*, V. 96, No. 1, Jan.-Feb. 1999, pp. 149-159.